inorganics

MDPI

Article

In Vitro Biological Activity of α-Diimine Rhenium Dicarbonyl Complexes and Their Reactivity with Different Functional Groups

Kevin Schindler [1], Justine Horner [1,2], Gozde Demirci [1], Youri Cortat [1], Aurélien Crochet [1], Olimpia Mamula Steiner [2] and Fabio Zobi [1,*]

[1] Department of Chemistry, Fribourg University, Chemin Du Musée 9, 1700 Fribourg, Switzerland
[2] Haute école d'ingénierie et d'architecture HEIA-FR, University of Applied Sciences of Western Switzerland, HES-SO, Pérolles 80, 1700 Fribourg, Switzerland; olimpia.mamulasteiner@hefr.ch
* Correspondence: fabio.zobi@unifr.ch

Abstract: Cancer remains one of the leading causes of death worldwide. The interest in organometallic complexes as anticancer drug candidates continues to be pivotal for many researchers. Initially underestimated for their therapeutic potentials, rhenium complexes are now slowly gaining momentum. While tricarbonyl complexes of rhenium are widely investigated, dicarbonyl derivatives of the *cis*-$[Re(CO)_2]^+$ core remain largely unexplored. In this study, we tested in vitro a variety of rhenium dicarbonyl complexes for their activity towards three cancer cell lines (A549, MCF-7 and HCT116) and one healthy cell line (HEK293). The most lipophilic compounds showed, like the tricarbonyl species, good activity against specific cancer lines (IC_{50} = 1.5–2.5 μM); however, the same were also toxic towards healthy cells. In order to understand these differences, we performed a reactivity study of *cis*-$[Re(CO)_2(NN)]^+$ species (where NN = diimine) with biologically relevant functional groups (-COOH, -NH_2, -SH and aromatic nitrogen-based ligands) and compared the chemistry to what is known for the *fac*-$[Re(CO)_3]^+$ core. Overall, we found that the rhenium dicarbonyl complexes only show good reactivity with aromatic nitrogen-based ligands. The reaction of *cis*-$[Re(CO)_2(NN)]^+$ species with common bio-functional groups leads, rather, to the formation of bis-diimine dicarbonyl complexes (*cis*-$[Re(CO)_2(NN)_2]^+$) as the major by-product.

Keywords: rhenium; dicarbonyl; anticancer agent; diimine ligands

Citation: Schindler, K.; Horner, J.; Demirci, G.; Cortat, Y.; Crochet, A.; Mamula Steiner, O.; Zobi, F. In Vitro Biological Activity of α-Diimine Rhenium Dicarbonyl Complexes and Their Reactivity with Different Functional Groups. *Inorganics* **2023**, *11*, 139. https://doi.org/10.3390/inorganics11040139

Academic Editor: Vladimir Arion

Received: 27 February 2023
Revised: 14 March 2023
Accepted: 21 March 2023
Published: 24 March 2023

1. Introduction

In the biomedical field, organometallic complexes are well-established anticancer agents, with the classical cisplatin and its derivatives commonly used in chemotherapy [1]. Although their efficiency has been proven, the development of new products and the understanding of their mode of action would allow the progression of treatment options and would undoubtedly accelerate the effectiveness of cancer treatment therapies [1–3]. Lately, the study of organometallic complexes has departed from solely fighting cancer and has been proposed as new solutions to the problems posed by bacterial resistance to antibiotic treatments [4]. Largely studied, owing to their photophysical and photochemical properties, and valuable in many applications such as bioimaging [5,6], luminescence [7,8], radiolabeling [9] and in catalysis [10–13], several studies have now revealed the high potential of rhenium tricarbonyl complexes (*fac*-$[Re^I(CO)_3]^+$) as antimicrobial [14–22], anticancer [23–32] and even recently as anti-COVID agents [33]. The mechanisms of action underlying the antibacterial and anticancer properties of *fac*-$[Re^I(CO)_3]^+$ species are numerous and not yet fully elucidated. However, it is very likely that interactions between these complexes and targeted biomolecules such as proteins or DNA are involved [23,24,26–32]. These interactions could be influenced by the stereochemistry of the complexes, as many studies have already highlighted the intrinsic role of metal compound chirality in biological activity [34–37].

In comparison with *fac*-$[Re^{I}(CO)_3]^+$ species, studies for anticancer properties of rhenium dicarbonyl complexes (*cis*-$[Re^{II}(CO)_2]^{+/2+}$) are extremely rare. Rossier et al. tested different metal complexes (Pt, Ru and Re) towards MCF-7 breast cancer cells. The *cis*-$[Re^{II}(CO)_2Br_2(HCCbpy)]$ complex (where HCCbpy is 4-ethynyl-2,2′-bipyridine) showed the greatest cytotoxic activity with an IC_{50} value of 1.4 μM (compared with 3.7 μM for cisplatin) [38]. Wilson and coworkers evaluated a series of water-soluble rhenium tricarbonyl complexes as photoactivated anticancer agents against various cancer cell lines. The products from the photoactivation of the tricarbonyl complexes may result in the formation of the dicarbonyl analogs. However, synthetically produced dicarbonyl complexes only showed moderate cytotoxicity, which suggests additional cell death mechanisms (such as $^1O_2$ and/or CO release) [39]. Metzler-Nolte and Godoy described a series of dicarbonyl cyrhetrenyl-bearing phosphine ligands and tested them towards cancer cell lines. A moderate biological activity was observed only with the most lipophilic compound [40], as was also the case with $[Re(CO)_2(NN)(PR_3)(Cl)]$ complexes (where NN = diimine and PR_3 are water-soluble phosphorous ligands), reported by Schutte-Smith and coworkers [41].

Our group has been interested in the synthesis of tri- and dicarbonyl rhenium complexes and in their applications in several medicinal areas, such as anticancer [38,42] and antibacterial agents [43,44] and CO-releasing molecules (CORMs) [45–47]. While the chemistry of *fac*-$[Re^{I}(CO)_3]^+$ species containing diimine ligands is well-established, the chemistry and biological applications of *cis*-$[Re^{II}(CO)_2]^{2+}$ and *cis*-$[Re^{I}(CO)_2]^+$ complexes are virtually unexplored. Thereby, in the recent years we have started investigating rhenium dicarbonyl chemistry and we recently presented a new synthetic route to aerobically stable and substitutionally labile α-diimine dicarbonyl rhenium(I) complexes with only π- and σ-donor ligands [48]. These new complexes were prepared from the $[Re(CO)_2(diimine)Br_2]^-$ anion by substitution of bromide with several monodentate, aromatic amino-type ligands. The dissociative substitution mechanism proceeded via a rearrangement involving a pentacoordinate intermediate, leading to the formation of different isomers in solution [48]. Due to the lack of data on the biological activity of *cis*-$[Re^{II}(CO)_2]^{+/2+}$ species, we decided to test such complexes in different cancer cell lines. Therefore, in this study, we describe the in vitro anticancer activity of several α-diimine rhenium dicarbonyl complexes and their reactivity with different functional groups of biological relevance. Where possible, their chemistry is compared with what is known for the *fac*-$[Re(CO)_3]^+$ core. We focused on α-diimine complexes, as diimine ligands are able to stabilize the *cis*-$[Re^{II}(CO)_2]^{+/2+}$ [48]. The same ligands are also commonly used in tricarbonyl rhenium chemistry, and the resulting metal complexes represent the vast majority of species tested for their biological activity to date [23,24,31]. Newer platinum complexes with modified diimine ligands are also being developed to improve efficacy and reduce toxicity [49–51].

2. Results and Discussion

Biological Activity of Rhenium Dicarbonyl Complexes

We started our study by testing rhenium dicarbonyl complexes previously published by our group (**1–5**, Scheme 1) against three cancer cell lines (A549, MCF-7 and HCT116) and one healthy cell line (HEK293). Table 1 presents the antiproliferative activity results of all tested compounds. Complexes of formula $[Re^{I}(CO)_2(NN)LL']^n$ (where NN = bipyridine type, L or L′ = monodentate ligands and n = 0 or +1, **1a–5a** and **2b–5b**, Scheme 1) showed no appreciable activity towards cancer cells. Only the more lipophilic complex, **1b**, exhibited activity towards MCF-7 cells with an IC_{50} value of 2.3 μM. This complex, however, was also toxic against healthy HEK293 cells (IC_{50} value of 3.0 μM). The general lack of activity of these species led us to evaluate two possibilities. On the one hand, we considered the possibility that the complexes may not be internalized by cancer cells, and, on the other hand, that the same compounds may lack reactivity towards common biological functional groups. An examination of the published contributions on anticancer *fac*-$[Re(CO)_3]^+$ complexes generally indicates that the cytotoxicity of the compounds positively correlates with lipophilic properties of the species [52–56], which are associated with an improved passive

cellular uptake. To address the first question (cellular internalization), we decided to prepare a *cis*-[Re(CO)$_2$-BODIPY] derivative in order to exploit the fluorescence properties of the chromophore and monitor the cellular uptake. We thus prepared a BODIPY-containing 2,2′-bipyridyl group according to Li et al. [57], and reacted the diimine with our 16 electron $[Re^{III}(CO)_2Br_4]^-$ precursor. Although low-yielding, the desired BODIPY complex was obtained. After HPLC purification, we were able to obtain single crystals suitable for X-ray diffraction (XRD) by slow diffusion of pentane into a CH_2Cl_2 (DCM) solution of the complex (Figure 1). Unfortunately, the fluorescence of the parent BODIPY ligand was drastically attenuated (by more than two orders of magnitude) by the coordination of the heavy Re atom, and we could not proceed with the intended fluorescent cellular internalization experiments. Here, it should be mentioned that the same quenching effect was previously noted with similar *fac*-[Re(CO)$_3$]$^+$ derivatives bearing pendant BODIPY chromophores directly bound to the diimine system [58–60].

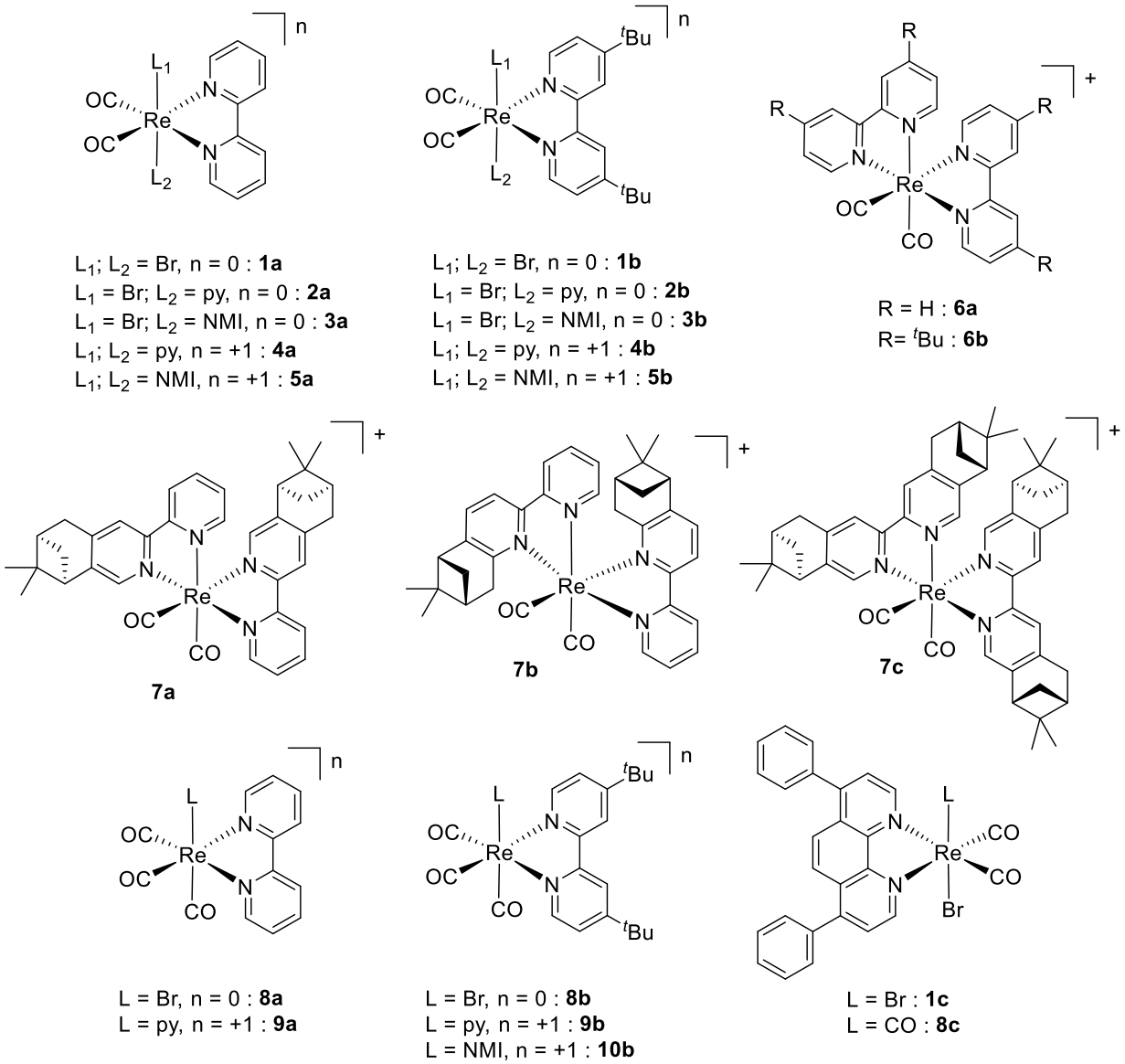

Scheme 1. Structures and numberings of rhenium di- and tri-carbonyl complexes tested in this study towards different cancer cell lines.

Table 1. IC_{50} values (in μM) of complexes **1–10** towards A549, MCF-7 and HCT116 cancer cell lines and HEK293 healthy human embryonic kidney cells.

Compounds	A549	MCF-7	HCT116	HEK293	Reference [a]
1a	>10	>10	>10	>10	[61]
1b	>10	2.3	>10	3.0	[48]
1c	>10	3.5	6.2	1.5	[61]
2a	>10	>10	>10	>10	[61]
2b	>10	>10	>10	>10	[48]
3a	>10	>10	>10	>10	[61]
3b	>10	>10	>10	>10	[48]
4a	>10	>10	>10	>10	[61]
4b	>10	>10	>10	>10	[48]
5a	>10	>10	>10	>10	[61]
5b	>10	>10	>10	>10	[48]
6a	>10	>10	>10	>10	
6b	3.3	4.1	1.5	0.5	
7a-1	>10	>10	>10	1.2	
7a-2	>10	>10	4.5	1.5	
7b-1	>10	>10	>10	9.8	
7b-2	>10	>10	>10	3.9	
7c-1	4.4	7.6	3.6	1.0	
7c-2	4.4	9.6	4.0	1.1	
8a	>10	>10	>10	>10	[44]
8b	9.7	7.1	6.3	4.9	[44]
8c	>10	8.2	6.9	>10	[61]
9a	>10	>10	>10	>10	[43]
9b	>10	>10	>10	8.8	[43]
10b	>10	>10	>10	>10	[43]

[a] Previously published compound. Note that none of the complexes in the table were previously tested for their biological activity.

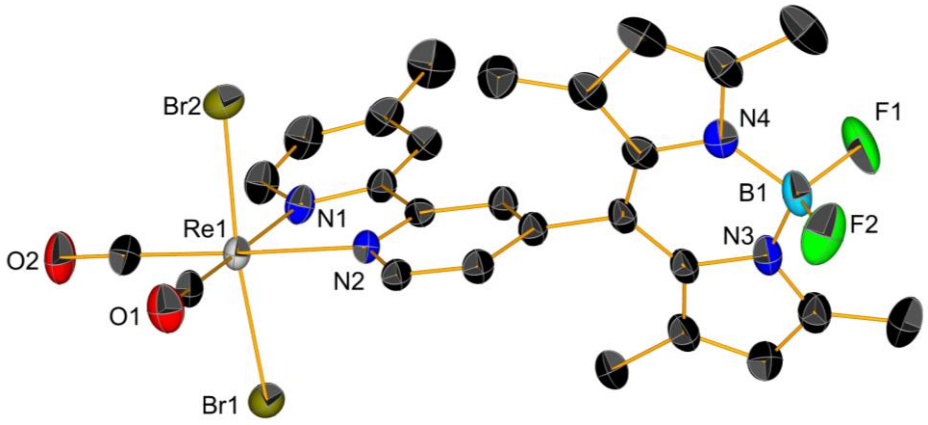

Figure 1. The ORTEP representation of crystal structure of the [$Re(CO)_2$-BODIPY] derivative. Thermal ellipsoids are at 30% probability. Hydrogen atoms are omitted for clarity.

We next moved to address the second question, and we explored the reactivity of the *cis*-$[Re^{I}(CO)_2]^+$ rhenium dicarbonyl species with various functional groups of biological relevance (-COOH, $-NH_2$, -SH and aromatic nitrogen-based ligands). Similar active anticancer *fac*-$[Re^{I}(CO)_3]^+$ rhenium tricarbonyl species act by different mechanisms of action, which include mitochondrial [62–66] or enzymatic inhibition [67] and DNA interaction [18,68–70]. Direct coordination of the complex to amino acid residues of proteins, or to DNA bases, is often evoked as a possible step in the mechanism of action of the complexes [23,24,26–32]. We reasoned, therefore, that the lack of activity of *cis*-$[Re^{I}(CO)_2]^+$ complexes **1–5** (Scheme 1) may be related to a lack of reactivity with available biological coordinating groups.

For the reactivity study, we selected the [Re(CO)$_2$(^{t}Bu$_2$bpy)Br(py)] complex (**2b**, Scheme 1) as a model compound (where ^{t}Bu$_2$bpy = 4,4′-di-*tert*-butyl-2,2′-bipyridine). The first step in this analysis involved the solvation of **2b** in a coordinating solvent such as methanol or water. When the rhenium complex was dissolved in methanol in the presence of one molar equivalent of silver trifluoromethanesulfonate, the substitution of the bromide ligand with the methanol was observed (by HPLC-MS), leading to the expected [Re(CO)$_2$(^{t}Bu$_2$bpy)(MeOH)(py)]$^+$ cation (Figure 2). Surprisingly, under the same reaction conditions (RT, 24 h) when water was used instead of methanol, no appreciable solvation of **2b** was noted as demonstrated by MS and HPLC-MS. By increasing the mixture temperature up to 80 °C, the unexpected [Re(CO)$_2$(^{t}Bu$_2$bpy)(OReO_3)(py)] complex (**11**) was isolated. Single crystals suitable for XRD analysis were obtained by layering pentane on the top of a solution of deuterated DCM. The X-ray structure shows isomerization of the starting product, leading to the *cis*,*cis*,*cis*-isomer (Figure 2). Despite many synthetic attempts, the substitution of the bromide ligand with water in **2b** could not be analytically established with confidence.

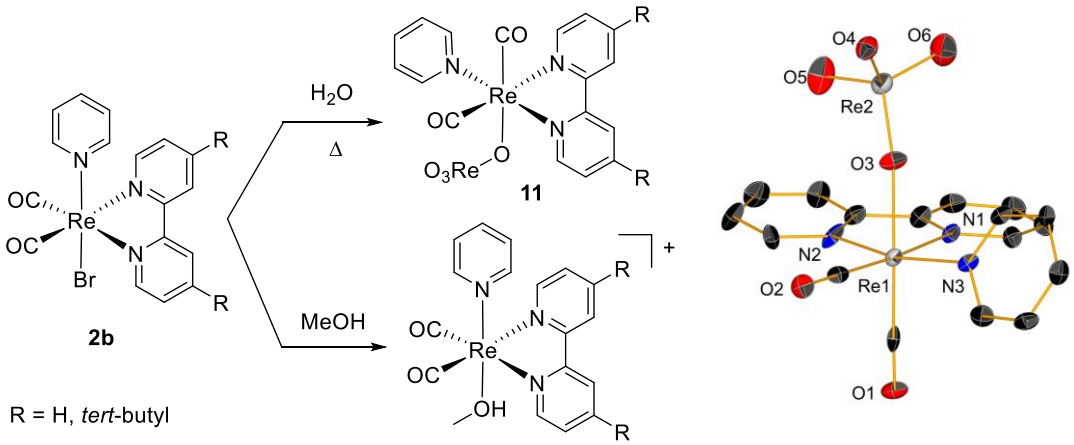

Figure 2. Solvated products from **2b** in methanol and water leading, respectively, to the [Re(CO)$_2$(bpy)(MeOH)(py)]$^+$ and [Re(CO)$_2$(bpy)(ReO_4)(py)] complexes. The ORTEP representation of crystal structure of **11** is shown to the right. Thermal ellipsoids are at 30% probability. Hydrogen atoms are omitted for clarity.

The next step of this investigation consisted of studying the reaction between **2b** various functional groups (carboxylic acids, amines and thiols) as ligands of biological relevance. At room temperature, over a prolonged time (2 days), no reaction was observed for all ligands tested (Figure 3). However, by heating the reaction mixture, a single major decomposition product, [Re(CO)$_2$(^{t}Bu$_2$bpy)$_2$](ReO_4) (**6b**), was recovered (Figure 3). The cation was equivalent to the set of complexes introduced by Meyer and Sullivan in 1983 [71,72]. These compounds, however, were prepared in the solid state by heating *fac*-[Re(CO)$_3$(NN)L] precursors with a large excess of melted NN ligand. Their luminescent properties were studied later along a series of molecules including *cis*-cis- and *cis-trans*-[Re(CO)$_2$(PP)(NN)] species (where PP = bidentate phosphine ligand), and exhibited low lifetimes (25 and 126 ns) and low quantum yields (ca. 0.0017 and 0.0032) for the bipyridine and phenanthroline ligands, respectively [72]. With reference to the same functional groups, the reactivity of rhenium dicarbonyl complexes was markedly different from that of closely related tricarbonyl species. The latter *fac*-[Re(CO)$_3$]$^+$ core reacted well with carboxylic acids [73–75], amines [76–78], aniline [79] and thiols [80,81], with several species also crystallographically characterized.

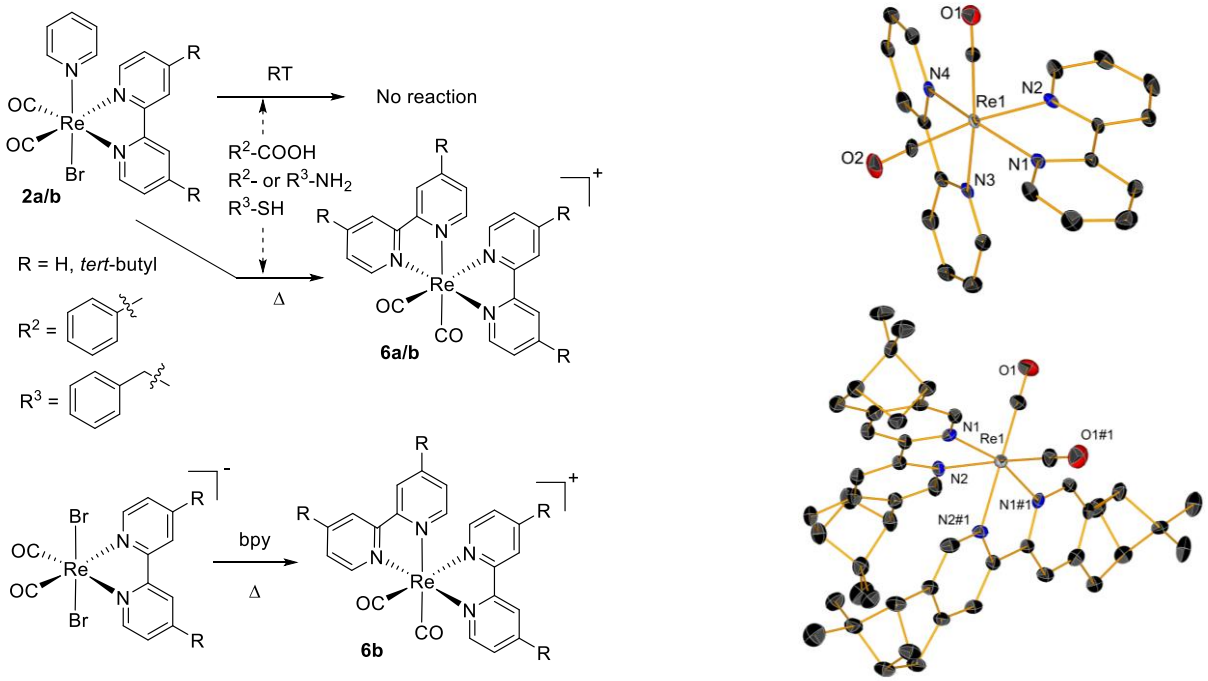

Figure 3. (**Top left**): schemes of the reactions of **2a/b** with benzoic acid, aniline, benzylamine and phenylmethanethiol. (**Bottom left**): scheme depicting the general direct synthesis of $[Re(CO)_2(NN)_2]^+$ cations (where NN is bpy- or pinbpy-type ligands). (**Right**): ORTEP representations of crystal structures of **6a** and **7c** cations. Thermal ellipsoids are at 30% probability. Hydrogen atoms are omitted for clarity.

Having accessed the $[Re(CO)_2(^tBu_2bpy)_2]^+$ cation in solution, we decided to attempt the preparation of similar species under more controlled reaction conditions. Boiling the $[Re(CO)_2(bpy)Br_2]$ complex (**1a**) with one molar equivalent of bipyridine in toluene only gave the desired cation in poor yield. On the other hand, the same reaction performed starting with the one-electron reduced species of **1a**, i.e., the $[Re(CO)_2(bpy)Br_2]^-$ anion (**1a***) [48], led to a much faster reaction and better yield, giving the $[Re(CO)_2(bpy)_2]^+$ cation (**6a**). Complex **6a** was purified by reverse-phase semi-preparative HPLC, and suitable crystals for X-ray diffraction were grown by layering pentane on a solution of deuterated DCM. The structure revealed the formation of perbromate as the counterion of the rhenium complex. We then pursued the same reaction with three chiral pinene diimine ligands [82], namely: (6R,8R)-7,7-dimethyl-3-(pyridin-2-yl)-5,6,7,8-tetrahydro-6,8-methanoisoquinoline ((-)-4,5-pinbpy), (5R,7R)-6,6-dimethyl-2-(pyridin-2-yl)-5,6,7,8-tetrahydro-5,7-methanoquinoline ((-)-5,6-pinbpy) and (6R,6′R,8R,8′R)-5,5′,6,6′,7,7′,8,8′-Octahydro-7,7,7′,7′-tetramethyl-3,3′-bi-6,8-methanoisoquinoline ((-)-bis-4,5-pinbpy). The $[Re(CO)_2(pinbpy)Br_2]^-$ starting anions were synthesized following the procedure developed by our lab for similar bipyridine complexes and used without further purifications because of the instability of these species in solutions [48]. The $[Re(CO)_2(pinbpy)Br_2]^-$ precursors were reacted in dry toluene with one molar equivalent of the same pinbpy diimine type ligands at 100 °C overnight, yielding the corresponding $[Re(CO)_2(pinbpy)_2]^+$ cations (**7a**: (-)-4,5-pinbpy; **7b**: (-)-5,6-pinbpy; **7c**: (-)-bis-4,5-pinbpy). They were similarly purified as described for **6a** and separated in two fractions of enriched stereoisomers. The first fraction of each complex contained the most polar stereoisomers (e.g., **7a-1**, see ESI), and the second one the less polar stereoisomers (e.g., **7a-2**, see ESI). These bis-diimine-based cationic complexes were tested in vitro for their biological activity towards the same cancer cell lines mentioned above. The complexes **6** and **7** showed, in general, higher antiproliferative activity than the first set of dicarbonyl compounds tested herein (i.e., **1–5**). The most active compound (**6b**) exhibited an IC_{50} value of 1.5 μM towards HCT116 cells. However, its toxicity against healthy

HEK293 cells was higher (0.5 μM). The different stereoisomers showed a similar activity, except for complex **7b**, where **7b-2** exhibited greater antiproliferative activity than **7b-1** towards A549, HCT116 and HEK293.

Because the reaction of the $[Re(CO)_2(^tBu_2bpy)Br(py)]$ complex **2b** with -COOH, $-NH_2$ and -SH functional groups did not lead to new products, we decided to perform similar reactions but starting from the $[Re^I(CO)_2(^tBu_2bpy)Br_2]^-$ precursor (**1b***, i.e., the one-electron reduced species of **1b**). Reactions were performed under inert conditions. No substitution reaction of the complex was observed with secondary and tertiary amines (diisopropylamine, diethylamine and trimethylamine). However, when **1b*** was reacted with benzylamine (bza, a primary amine model ligand), MS analysis of the reaction mixture indicated the substitution of the two coordinated bromide ions in **1b*** by bza, leading to the di-substituted amino $[Re(CO)_2(^tBu_2bpy)(bza)_2]^+$ compound (**12**). The crude product of this reaction was purified on aluminum oxide, but, surprisingly, the XRD structure of the eluted product revealed the formation of the dicarbonyl $[Re(CO)_2(bza)_4]^+$ cation (**13**) with four benzylamine ligands (Figure 4). As we never detected **13** in the reaction mixture, we suppose that it is probably formed by the decomposition of **12** on aluminum oxide. No further analysis was performed on **13**. In order to further explore this chemistry, we then reacted the 16 electron $(Et_4N)[Re^{III}(CO)_2Br_4]$ complex [83] with benzylamine, imidazole and pyridine. The crude products from these reactions were difficult to analyze and purify because they were too polar for normal phase chromatography and unstable on reverse phase HPLC.

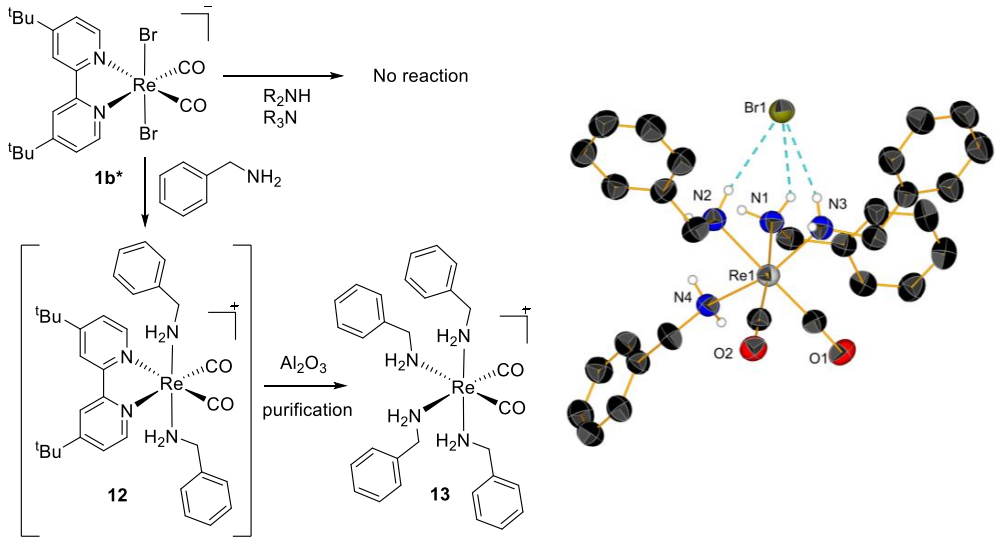

Figure 4. (**Left**): schemes of the reactions of **1b*** with model primary, secondary and tertiary amines. (**Right**): ORTEP representations of crystal structures of rhenium complex **13** obtained from the decomposition of **12**. Thermal ellipsoids are at 30% probability. Hydrogen atoms are omitted for clarity.

We finally tested the reactivity of **2b** with aromatic nitrogen-based ligands. We selected acyclovir (**acv**) as a nucleoside analogue for our study and the amino acid L-histidine (**his**). Acyclovir is an antiviral medication primarily used for the treatment of herpes simplex virus infections [84]. Contrary to carboxylic acids, amines and thiols, acyclovir displays coordination affinity for the rhenium dicarbonyl complex. The reaction of **2b** with **acv** as monitored via analytical HPLC was completed after ca. 100 h (4 days). The crude $[Re(CO)_2(^tBu_2bpy)(acv)(py)]Br$ product (**15**) was purified by reverse phase semi-preparative HPLC. Complex **15** was stable, and it could be characterized by NMR (Figure 5). Attempts to obtain crystals of **15** suitable for XRD were only partially successful. The XRD data confirmed the structure of the compound (Figure 5), but due to the progressive deterioration of the crystal, the same data could not be fully refined. Similarly, **2b** reacted

rapidly with **his**, giving the $[Re(CO)_2(^tBu_2bpy)(his)(py)]^+$ cation (**16**). This was isolated as a PF_6^- salt following purification by reverse phase semi-preparative HPLC. Here, it should be noted that, while all analytical data point to the formation of **16**, we could not unambiguously assign the coordination mode of **his** to **2b**. In solution, the NMR spectrum of the complex (see ESI) was rather broad, a fact that we attribute either to partial decomposition of the complex or to a dynamic equilibrium between the *cis-cis-cis* and *cis-cis-trans* isomers as previously observed [48]. We suggest coordination of **his** via the imidazole ring, based on the collected evidence of this study and the fact that complexations with other amino acids, such as glycine, only gave analytical traces (observed by HPLC-MS) of possible interaction with **2b**, and the fact that carboxylic acid and primary amines did not show affinity for the *cis*-$[Re(CO)_2]^+$ core. Overall the reactivity of the *cis*-$[Re(CO)_2]^+$ core (i.e., with aromatic nitrogen-based ligands) is comparable to that of the *fac*-$[Re(CO)_3]^+$, with several studies supporting the interaction of the latter core with guanines [85–89] and histidine [90–96].

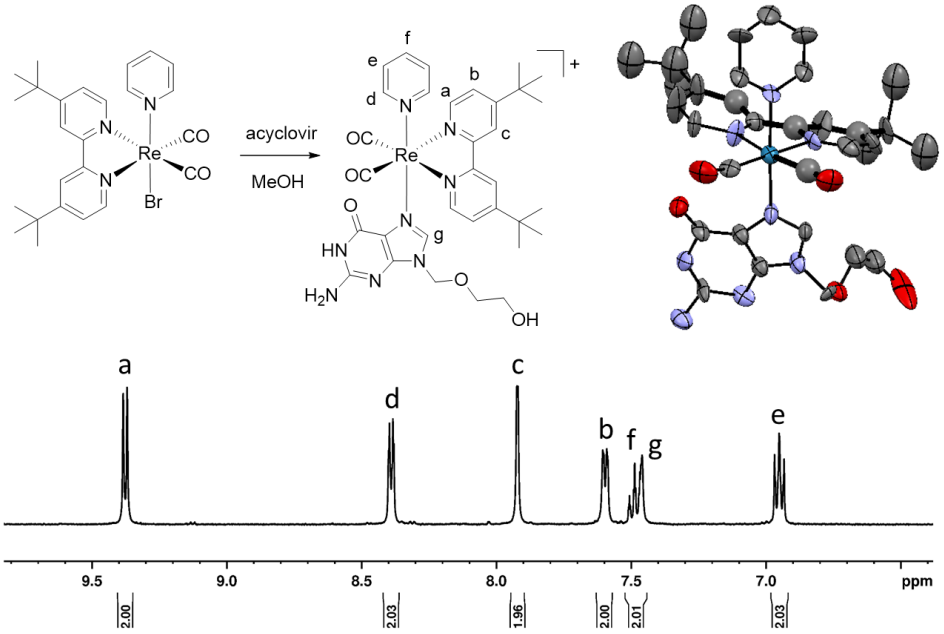

Figure 5. Aromatic region of NMR spectrum (in CD_2Cl_2) of **15** cation and its structure, based on XRD data. Letters in the NMR spectrum refer to hydrogen resonance signals of **15** cation as of scheme.

3. Materials and Methods

3.1. Reagents and Chemicals

All reagents and solvents were acquired from common sources and employed without further purifications. Complexes **1a** [97] and **1c**, **2a**, **3a**, **4a**, **5a** and **1c** [61], as well as **1b**, **2b**, **3b**, **4b** and **5b** [48] were synthesized according to published procedures. BODIPY ligand was obtained according to established methods [57]. Chiral ligands (-)-4,5-pinbpy, (-)-5,6-pinbpy [82] and (-)-bis-4,5-pinbpy [98] were prepared following known procedures. Each (TDAE)$[Re^I(CO)_2(pinbpy)Br_2]_2$ synthon was synthesized via a previously published method for rhenium dicarbonyl complexes bearing α-diimine ligand [48]. All molecules were prepared under inert atmosphere (Ar) using dry solvents, unless otherwise noted. Dulbecco's Modified Eagle Medium (DMEM) (with L-glutamine and glucose), L-glutamine penicillin/streptomycin (l-glu pen-strep) and trypsin-EDTA were purchased from Pan, Biotech. Thiazolyl blue tetrazolium bromide (MTT) was provided by Thermoscientific–Acros. Fetal bovine serum (FBS) and phosphate-buffered saline (PBS, 1X) solution was obtained from Gibco. Ninety-six-well plates were purchased from Nuncklon–Thermo. MCF-7–breast cancer cell line, HCT116–human colon cancer cell line, A549–lung carcinoma

cell line and HEK293–human embryonic kidney cells were kindly gifted from Prof. David Hoogewijs, Department of Medicine, University of Fribourg, Switzerland.

3.2. Instruments and Analysis

NMR spectra were measured on a Bruker Advance III 400 MHz. The corresponding ^{1}H chemical shifts were reported relative to residual solvent protons. Mass analyses were performed either using ESI-MS or a Bruker FTMS 4.7-T Apex II in positive mode. UV-Vis spectra were measured on a Jasco V730 spectrophotometer. IR spectra were recorded on a Bruker TENSOR II with the following parameters: 16 scans for background and 32 scans for sample with a resolution of 4 cm^{-1} in the 4000 to 600 cm^{-1} region. Analytical HPLCs were performed with a Merck Hitachi L-7000 system, which comprised a pump L-7100 and a UV-detector L-7400. For preparative HPLC, a column Macherey-Nagel Nucleodur C18 HTec (5 µm particle size, 110 Å pore size, 250 × 21 mm) was used. Pure water (A), pure methanol (B) and pure acetonitrile (C) were, respectively, used as solvents. The compounds were analyzed using the gradient described in the synthetic procedures, the flow rate was set to 5 mL min^{-1} and the compounds were detected at 260 nm. Single crystal diffraction data collection was performed on a Stoe IPDS2 diffractometer (CuKα1 (λ = 1.5406 Å)) equipped with a cryostat from Oxford Cryosystems. The structures were solved with the ShelXT structure solution program using Intrinsic Phasing and refined with the ShelXL refinement package using Least Squares minimization [99,100]. All crystal structures were deposited at the Cambridge Crystallographic Data Centre. CCDC numbers 2244186-2244190 contain the Supplementary Crystallographic Data for this paper. For determination of the antiproliferative activity, Tecan-Spark 10 M was used with SparkControl program.

3.3. In Vitro Antiproliferative Activity Assay

Impact of the prepared complexes on the viability of MCF-7, HCT116, A549 and HEK293 cell lines was evaluated using the standard MTT assay. The cells were cultured in DMEM complete medium supplemented with 10% (v/v) FBS and 1% (v/v) l-glu pen-strep in a 5% CO_2-humidified incubator at 37 °C and subcultured regularly. For viability tests, cells were seeded at a density of 1 × 10^4 cells for cancer cells and 1.25 × 10^4 for HEK293 cells in 200 µL complete medium in each well and incubated at 37 °C in 5% CO_2 atmosphere. After 24 h, complexes in DMSO were injected with fresh medium into the wells at a concentration between 0.63 and 10 µM. In the highest concentration, the ration of the DMSO was arranged to 1% v/v. Then, after 24 h incubation, the cell viability was assessed using MTT colorimetric assay. Cells that were not exposed with complexes were used as controls. One hundred percent viability was assumed for the control cells. The relative cell viability was calculated by the following formula:

$$cell\ viability(\%) = \frac{Absorbance\ (complex)}{Absorbance\ (control)} \times 100 \quad (1)$$

Statistical analyses of the cytotoxicity of complexes were conducted by using ordinary one-way ANOVA analysis of variance followed by multiple Dunnett's comparison tests of GraphPad Prism 8.4.2 software package. All measurements were expressed as mean values ± standard deviation (SD) based on 5 replicas. $p < 0.05$ was accepted as a statistically significant difference. Statistical significance: (*) $p < 0.0332$, (**) $p < 0.021$, (***) $p < 0.0002$ and (****) $p < 0.0001$. For IC50 calculation, nonlinear regression analysis followed by variable slope was used.

3.4. Synthetic Procedures

[Re(CO)$_2$-BODIPY]. (Et_4N)[$Re^{III}(CO)_2Br_4$] (83.1 mg, 0.120 mmol) and BODIPY (50 mg, 0.120 mmol) were stirred at RT in DCM (25 mL) for 2.5 h and the solvent was then removed under reduced pressure. The crude solid was purified by flash column chromatography on silica (eluent: DCM/pentane 2:1 → 1:0). The second fraction was isolated as a pink

solid once dried. Yield: 13.9 mg, 0.0170 mmol, 14%. IR (cm^{-1}), ν_{CO}: 2001, 1864. NMR: not available (paramagnetic compound).

[Re(CO)$_2$(bpy)$_2$](BrO$_4$) (6a). Degassed complex (TDAE)[Re(CO)$_2$(bpy)Br$_2$]$_2$ (24.5 mg, 37.2 μmol in Re) and 2,2′-bipyridine (5.8 mg, 37.2 μmol) were dissolved in dry toluene (8 mL). The mixture was heated to 100 °C overnight. The solvent was removed under reduced pressure. The residue was dissolved in H_2O/MeOH 1:2 (5 mL). A solution of KPF_6 (6.8 mg, 37.2 μmol) in H_2O/MeOH 1:1 (2 mL) was added dropwise to the Re solution in order to exchange the counterion (this ion exchange did not work properly, according to the crystal structure). The mixture was filtered and purified by HPLC semi preparative using the following gradient: 0–5 min (65% A), 5–35 min (65% A → 0% A), 35–45 min (100% B). The desired fraction (retention time: ca. 20 min) was collected and dried by lyophilization yielding to a dark red solid (**6a**). Yield: 4.9 mg, 7.0 μmol, 19%. Single crystals suitable for X-ray diffraction were grown by layering pentane on a CD_2Cl_2 solution of the compound. IR (cm^{-1}), ν_{CO}: 1902, 1822. UV-Vis (MeOH), λ_{max} [nm]: 482, 397, 287, 245. ^{1}H NMR (400 MHz, CD_2Cl_2, ppm): δ = 9.48 (d, J = 5.7 Hz, 2H), 8.61 (d, J = 8.2 Hz, 2H), 8.55 (d, J = 8.2 Hz, 2H), 8.11–8.17 (dt, 2H), 8.06 (dt, J = 8.2, 4.6 Hz, 2H), 7.57 (ddd, J = 7.4, 5.8, 1.3 Hz, 2H), 7.36 ppm (d, J = 4.4 Hz, 4H). ESI-MS (MeOH): m/z, 554.7 $[M]^+$.

[Re(CO)$_2$(^{t}Bu$_2$bpy)$_2$](PF$_6$) (6b). Degassed complex (TDAE)[Re(CO)$_2$(^{t}Bu$_2$bpy)Br$_2$]$_2$ (52.8 mg, 68.5 μmol in Re) and ^{t}Bu$_2$bpy (18.4 mg, 68.5 μmol) were dissolved in dry toluene (20 mL). The mixture was heated to 100 °C overnight. The solvent was removed under reduced pressure. The residue was dissolved in MeOH (10 mL). A solution of KPF_6 (12.6 mg, 68.5 μmol) in H_2O/MeOH 1:1 (2 mL) was added dropwise to the Re solution in order to exchange the counterion. The mixture was filtered and purified by HPLC semi preparative using the following gradient: 0–5 min (65% A), 5–35 min (65% A → 0% A), 35–45 min (100% B). The desired fraction (retention time: ca. 20 min) was collected and dried by lyophilization yielding to a dark red solid (**6b**). Yield: 11.1 mg, 12.0 μmol, 17%. IR (cm^{-1}), ν_{CO}: 1897, 1822. UV-Vis (MeCN), λ_{max} [nm]: 465, 387, 285, 248, 207. ^{1}H NMR (400 MHz, CD_3CN, ppm): δ = 9.29 (d, J = 6.1 Hz, 2H), 8.44 (d, J = 1.96 Hz, 2H), 8.38 (d, J = 1.71 Hz, 2H), 7.63 (dd, J = 2.20, 6.11 Hz, 2H), 7.35 (dd, J = 1.96, 5.99 Hz, 2H), 7.29 (dd, J = 0.43, 5.93 Hz, 2H), 1.50 (s, 18H), 1.33 (s, 18H). ESI-MS (MeOH): m/z, 779.1 $[M]^+$.

[Re(CO)$_2$(4,5-pinbpy)$_2$](PF$_6$) (7a). (TDAE)[Re^I(CO)$_2$(4,5-pinbpy)Br$_2$]$_2$ (76.1 mg, 0.0966 mmol in Re, 1 eq) and 4,5-pinbpy (25.4 mg, 0.101 mmol, 1.05 eq) were dissolved in dry toluene (20 mL). The mixture was stirred under inert atmosphere at 100 °C overnight. The solvent was evaporated. The solid residue (102.7 mg) was dissolved in a MeOH/H_2O mixture (2/1, 30 mL) and a solution of KPF_6 (27 mg, 0.147 mmol, 1.52 eq, in H_2O 1 mL + MeOH 1 mL) was added dropwise. The solution was stirred at RT for 10 min. The solvent was evaporated to collect the crude product as a dark red solid. The crude compound was then purified by HPLC semi preparative using the following gradient: 0–3 min (70% A), 3–45 min (70% A → 0% A), 45–70 min (100% B). Two red fractions were collected, so-called product **7a-1** (minor) between 32 and 37.2 min and so-called product **7a-2** (major) between 37.2 and 44 min. After solvent evaporation and drying, 9.5 mg of product **7a-1** and 22.0 mg of product **7a-2** were collected as red solids. Yields: 31.5 mg, 0.0357 mmol, 36.9%. IR (cm^{-1}), ν_{CO}: 1904, 1830. UV-Vis (MeOH), λ_{max} [nm]: 499, 393, 293. ^{1}H NMR (300 MHz, CD_2Cl_2, ppm): δ = 9.41–9.31 (m, 2H), 8.32 (dq, J = 8.3, 1.2 Hz, 2H), 8.08 (d, J = 12.9 Hz, 2H), 8.04–7.94 (m, 2H), 7.41 (dddd, J = 7.4, 5.9, 4.6, 1.4 Hz, 2H), 6.71 (d, J = 6.8 Hz, 2H), 3.14–2.84 (m, 4H), 2.62–2.48 (m, 2H), 2.42 (q, J = 5.5 Hz, 2H), 2.27–2.15 (m, 2H), 1.26 (s, 3H), 1.22 (s, 3H), 0.98 (dd, J = 43.0, 10.0 Hz, 2H), 0.52 (s, 3H), 0.14 (s, 3H). ESI-MS (MeOH): m/z, 742.9 $[M]^+$.

[Re(CO)$_2$(5,6-pinbpy)$_2$](PF$_6$) (7b). (TDAE)[Re^I(CO)$_2$(5,6-pinbpy)Br$_2$]$_2$ (0.129 mmol in Re, 1 eq) and 5,6-pinbpy (34.0 mg, 0.139 mmol, 1.05 eq) were dissolved in dry toluene (20 mL). The mixture was stirred under inert atmosphere at 100 °C overnight. The solvent was evaporated. The solid residue (134.4 mg) was dissolved in a MeOH/H_2O mixture (2/1, 20 mL) and a solution of KPF_6 (27 mg, 0.147 mmol, 1.14 eq, in H_2O 1 mL + MeOH 1 mL) was added dropwise. The solution was stirred at RT for 10 min. The solvent was

evaporated to collect the crude product as a dark red solid (155.4 mg). The crude compound was then purified by HPLC semi preparative using the following gradient: 0–3 min (70% A), 3–38 min (70% A → 0% A), 38–60 min (100% B). Two red fractions were collected, so-called product **7b-1** (minor) between 31 and 35 min and so-called product **7b-2** (major) between 36 and 42 min. After solvent evaporation and drying, 1.5 mg of product **7b-1** and 10.8 mg of product **7b-2** were collected as red solids. Yields: 12.3 mg, 0.0357 mmol, 10.8%. IR (cm^{-1}), ν_{CO}: 1915, 1839. UV-Vis (MeOH), λ_{max} [nm]: 481, 397, 300. ^{1}H NMR (300 MHz, CD_2Cl_2, ppm): δ = 9.49–9.41 (m, 2H), 8.13–8.08 (m, 2H), 7.96 (d, J = 8.1 Hz, 2H), 7.92–7.83 (m, 2H), 7.47 (dd, J = 8.1, 4.6 Hz, 2H), 7.38–7.29 (m, 2H), 2.78–2.71 (m, 2H), 2.59–2.55 (m, 3H), 2.50–2.38 (m, 2H), 1.80 (dp, J = 9.3, 3.1 Hz, 2H), 1.64 (d, J = 2.9 Hz, 1H), 1.22 (s, 3H), 1.16 (s, 3H), 1.01 (d, J = 10.1 Hz, 2H), 0.45 (s, 3H), 0.07 (s, 3H). ESI-MS (MeOH): *m*/*z*, 742.9 $[M]^+$.

[Re(CO)$_2$(bis-4,5-pinbpy)$_2$](PF$_6$) (7c). (TDAE)[Re^{I}(CO)$_2$(bis-4,5-pinbpy)Br$_2$]$_2$ (0.201 mmol in Re, 1 eq) and bis-4,5-pinbpy (73.9 mg, 0.215 mmol, 1.07 eq) were dissolved in dry toluene (40 mL). The mixture was stirred under inert atmosphere at 100 °C overnight. The solvent was evaporated. The solid residue (261.8 mg) was dissolved in a MeOH/H_2O mixture (2/1, 30 mL) and a solution of KPF_6 (47.7 mg, 0.259 mmol, 1.29 eq, in H_2O 1 mL + MeOH 1 mL) was added dropwise. The solution was stirred at RT for 10 min. The solvent was evaporated to collect the crude product as a dark red solid (294.5 mg). The crude compound was then purified by HPLC semi preparative using the following gradient: 0–1 min (70% A/30% C), 1–45 min (70% A → 0% A), 45–60 min (100% C). Two red fractions were collected, **7c-1** between 16 and 20 min and **7c-2** between 25 and 29 min. After solvent evaporation and drying, 15.4 mg of product **7c-1** and 15.8 mg of product **7c-2** were collected as red solids. Yields: 31.2 mg, 0.0687 mmol, 34.2%. IR (cm^{-1}), ν_{CO}: 1899, 1831. UV-Vis (MeOH), λ_{max} [nm]: 487, 398, 298. ^{1}H NMR (300 MHz, CD_3CN, ppm): δ = 8.74 (s, 2H), 7.99 (s, 2H), 7.93 (s, 2H), 6.58 (s, 2H), 3.06–2.99 (m, 4H), 2.90–2.82 (m, 6H), 2.69–2.59 (m, 2H), 2.50–2.34 (m, 2H), 2.27–2.20 (m, 2H), 2.18 (t, J = 5.5 Hz, 2H), 2.11–2.05 (m, 2H), 1.30 (s, 6H), 1.18–1.14 (m, 2H), 1.11 (s, 6H), 0.73 (d, J = 9.9 Hz, 2H), 0.60 (s, 6H), 0.38 (s, 6H). ESI-MS (MeOH): *m*/*z*, 931.1 $[M]^+$.

[Re(CO)$_2$(batho)Br$_2$] (1c). (Et$_4$N)[Re^{III}(CO)$_2$Br$_4$] (100 mg, 144 μmol, 1 eq) and bathophenanthroline (batho) (48 mg, 144 μmol, 1 eq) were dissolved in dry DCM (10 mL) and the reaction mixture was stirred under argon atmosphere for 3 h at RT. The solvent was removed by rotary evaporation and the crude product was purified by flash chromatography (pentane/EtOAc, 10:1) on silica. Brown solid, yield 34%. IR (cm^{-1}), ν_{CO}: 1999, 1848. Crystals suitable for X-ray diffraction were obtained by slow evaporation of a DCM solution of **1c**.

***fac*-(bromo)tricarbonylrhenium(I) (1c-8a-8b).** These compounds were synthesized according to the literature [44]. [Re(CO)$_5$Br] (100 mg, 246 μmol, 1 eq) and the diimine (246 μmol, 1 eq) were dissolved in toluene (2 mL) and refluxed (100 °C) overnight. The reaction mixture was cooled down to RT and the pale yellow, yellow and orange solid precipitates were isolated by filtration followed by washing with toluene (~10 mL). Pale yellow (**^{t}Bu$_2$bpy**), yellow (**bpy**) or orange (**batho**) solid, 87.3–92.1%.

***fac*-(py)tricarbonylrhenium(I) (9a-9b).** Bromo complex (<50 mg, 1 eq) and AgOTf (2 eq) were suspended in a solution of pyridine (25 eq) in MeOH (5 mL) and refluxed (55 °C) for 20 h. The reaction mixture was cooled down to RT, filtered and dried in vacuo. The crude product was purified by HPLC semi preparative using the following gradient: 0–5 min (75% A), 5–35 min (75% A → 50% A), 35–40 min (50% A), 40–45 min (100% B) for bpy, and 0–20 min (30% A), 20–30 min (100% B) for ^{t}Bu$_2$bpy. Pale yellow (^{t}Bu$_2$bpy) or yellow (bpy) solid, 58–59 %.

[Re(CO)$_3$(^{t}Bu$_2$bpy)(NMI)](OTf) (10b). [Re(CO)$_3$(^{t}Bu$_2$bpy)Br] (40 mg, 65 μmol, 1 eq) and AgOTf (33 mg, 130 μmol, 2 eq) were suspended in a solution of N-methylimidazole (NMI) (100 μL, 1.3 mmol, 25 eq) in MeOH (5 mL) and refluxed (55 °C) for 20 h. The reaction mixture was cooled down to RT, filtered and dried in vacuo. The crude product was suspended in H_2O (60 mL) and centrifugated. The liquid was decanted and this process was repeated two additional times. The resulting pale yellow solid was dissolved

in acetonitrile (5 mL) and the resulting solution was filtered and dried in vacuo. Pale yellow solid, 72 %.

[Re(CO)$_2$(^{t}Bu$_2$bpy)(acv)(py)](Br) (15). Complex **2b** (31 mg, 46.3 µmol) and acyclovir (10.5 mg, 46.3 µmol) were dissolved in methanol (10 mL). The mixture was heated to 75 °C for 4 days (ca. 100 h). The reaction was then cooled down to room temperature, KPF_6 (9.4 mg, 50.9 µmol, 1.1 eq.) was added and the solution was stirred for 15 min (this ion exchange did not work properly, according to the crystal structure). The mixture was filtered and purified by HPLC semi preparative using the following gradient: 0–5 min (70% A), 5–35 min (70% A → 0% A), 35–45 min (100% B). The desired fraction (retention time: ca. 21 min) was collected and dried by lyophilization yielding to a dark red solid (**15**). Yield: 5.2 mg, 5.8 µmol, 13%. IR (cm^{-1}), ν_{CO}: 1900, 1818. UV-Vis (MeOH), λ_{max} [nm]: 365, 303, 249. ^{1}H NMR (400 MHz, CD_2Cl_2, ppm): δ = 9.46 (d, J = 5.9 Hz, 2H), 8.47 (dd, J = 6.5, 1.4 Hz, 2H), 8.00 (d, J = 1.6 Hz, 2H), 7.68 (d, J = 6.0 Hz, 2H), 7.55–7.60 (tt, 1H), 7.54 (s, 1H), 7.03 (dt, J = 7.5, 6.7 Hz, 2H), 6.08 (br. s., 2H), 5.28 (s, 2H), 3.57–3.61 (t, 2H), 3.44–3.48 (t, 2H), 1.40 (s, 18H). ESI-MS (MeOH): *m/z*, 815.0 [M]$^+$.

[Re(CO)$_2$(^{t}Bu$_2$bpy)(his)(py)](PF$_6$) (16). Complex **2b** (25 mg, 37.3 µmol) and L-histidine (8.7 mg, 56.0 µmol, 1.5 eq.) were dissolved in methanol (10 mL). The mixture was heated to 75 °C for 55 h. The reaction was then cooled down to room temperature, KPF_6 (7.6 mg, 41.0 µmol, 1.1 eq.) was added and the solution was stirred for 15 min. The mixture was filtered and purified by HPLC semi preparative using the following gradient: 0–5 min (65% A), 5–35 min (65% A → 0% A), 35–45 min (100% B). The desired fraction (retention time: ca. 34 min) was collected and dried by lyophilization yielding to a dark orange solid (**15b**). Yield: 5.6 mg, 6.3 µmol, 17%. IR (cm^{-1}), ν_{CO}: 1894, 1813. ^{1}H NMR (400 MHz, CD_2Cl_2, ppm): δ = 9.07 (d, J = 6.11 Hz, 1H), 8.57 (d, J = 10.51 Hz, 2H), 8.23 (s, 1H), 7.99–8.10 (m, 2H), 7.65–7.78 (m, 1H), 7.59 (dd, J = 5.81, 9.60 Hz, 1H), 7.13–7.36 (m, 4H), 6.19–6.41 (m, 1H), 3.10–3.36 (m, 1H), 2.72–2.98 (m, 1H), 1.46 (d, J = 8.19 Hz, 9H), 1.37 (d, J = 5.75 Hz, 9H). ESI-MS (MeOH): *m/z*, 745.0 [M]$^+$.

4. Conclusions

In this study, we reported the synthesis, characterization and biological activity of a series of rhenium dicarbonyl complexes, including eight new complexes. Our in vitro biological evaluation revealed good toxicity towards three cancer cell lines (A549, MCF-7 and HCT116) for the most lipophilic compounds, but the same complexes were also toxic towards a healthy cell line (HEK293). These dicarbonyl complexes turned out to be less efficient anticancer molecules compared with tricarbonyl compounds. Further analysis revealed that the reactivity of rhenium dicarbonyl complexes was only high with aromatic nitrogen-based ligands, while reactions with other biologically relevant functional groups (-COOH, -NH$_2$, -SH) led to the formation of bis-diimine dicarbonyl complexes as the major by-product. We finally developed a straightforward synthetic route to obtain the bis-diimine [Re(CO)$_2$(NN)$_2$]$^+$ cations.

Supplementary Materials: The following supporting information can be downloaded at: https://www.mdpi.com/article/10.3390/inorganics11040139/s1, Figures S1–S7: 1H-NMR spectra of compounds; Figures S8–S14: IR spectra (solid state) of compounds; Figures S15–S20: UV-Vis spectra (in MeOH) of compounds; Figures S21–S27: ESI-MS spectra (in MeOH) of compounds; Figure S28–S31: Cytotoxicity graphs of compounds; Table S1: Crystallographic details of complexes.

Author Contributions: Conceptualization, F.Z.; methodology, K.S., J.H. and G.D.; formal analysis, K.S., J.H., G.D, Y.C. and A.C.; investigation, K.S., J.H. and G.D.; resources, F.Z. and O.M.S.; data curation, K.S., J.H. and G.D.; writing—original draft preparation, K.S.; writing—review and editing, all authors; supervision, F.Z. and O.M.S.; project administration, F.Z. and O.M.S.; funding acquisition, F.Z. and O.M.S. All authors have read and agreed to the published version of the manuscript.

Funding: This research was funded by the Swiss National Science Foundation (project# 200021_196967).

Data Availability Statement: All data available upon request.

Acknowledgments: David Hoogewijs and Darko Maric (Section of Medicine, University of Fribourg) are gratefully acknowledged for providing all cancer cell lines and allowing G.D. to conduct experimentation in their laboratory.

Conflicts of Interest: The authors declare no conflict of interest.

References

1. Cirri, D.; Bartoli, F.; Pratesi, A.; Baglini, E.; Barresi, E.; Marzo, T. Strategies for the Improvement of Metal-Based Chemotherapeutic Treatments. *Biomedicines* **2021**, *9*, 504. [CrossRef] [PubMed]
2. Siegel, R.L.; Miller, K.D.; Fuchs, H.E.; Jemal, A. Cancer statistics, 2022. *CA Cancer J. Clin.* **2022**, *72*, 7–33. [CrossRef] [PubMed]
3. Wang, Y.; Huang, H.; Zhang, Q.; Zhang, P. Chirality in metal-based anticancer agents. *Dalton Trans.* **2018**, *47*, 4017–4026. [CrossRef]
4. Nasiri Sovari, S.; Zobi, F. Recent Studies on the Antimicrobial Activity of Transition Metal Complexes of Groups 6–12. *Chemistry* **2020**, *2*, 418–452. [CrossRef]
5. Schrage, B.R.; Frisinger, B.R.; Schmidtke Sobeck, S.J.; Ziegler, C.J. Lipophilic $Re(CO)_3$pyca complexes for Mid-IR imaging applications. *Dalton Trans.* **2021**, *50*, 1069–1075. [CrossRef] [PubMed]
6. Raszeja, L.J.; Siegmund, D.; Cordes, A.L.; Güldenhaupt, J.; Gerwert, K.; Hahn, S.; Metzler-Nolte, N. Asymmetric rhenium tricarbonyl complexes show superior luminescence properties in live cell imaging. *Chem. Commun.* **2017**, *53*, 905–908. [CrossRef]
7. Herrick, R.S.; Wrona, I.; McMicken, N.; Jones, G.; Ziegler, C.J.; Shaw, J. Preparation and characterization of rhenium(I) compounds with amino ester derivatized diimine ligands. Investigations of luminescence. Crystal structures of Re(CO)3Cl(pyca-β-Ala-OEt) and Re(CO)3Cl(pyca-l-Asp(OMe)-OMe). *J. Organomet. Chem.* **2004**, *689*, 4848–4855. [CrossRef]
8. Saleh, N.; Srebro, M.; Reynaldo, T.; Vanthuyne, N.; Toupet, L.; Chang, V.Y.; Muller, G.; Williams, J.A.G.; Roussel, C.; Autschbach, J.; et al. enantio-Enriched CPL-active helicene–bipyridine–rhenium complexes. *Chem. Commun.* **2015**, *51*, 3754–3757. [CrossRef]
9. Rattat, D.; Schubiger, P.A.; Berke, H.G.; Schmalle, H.; Alberto, R. Dicarbonyl-Nitrosyl-Complexes of Rhenium (Re) and Technetium (Tc), A Potentially New Class of Compounds for the Direct Radiolabeling of Biomolecules. *Cancer Biother. Radiopharm.* **2001**, *16*, 339–343. [CrossRef]
10. Burzlaff, N.; Schenk, W.A. Chiral Rhenium Complexes of Functionalized Thioaldehydes. *Eur. J. Inorg. Chem.* **1999**, *1999*, 1435–1443. [CrossRef]
11. Faller, J.W.; Lavoie, A.R. Diastereoselective Synthesis and Electronic Asymmetry of Chiral Nonracemic Rhenium(V) Oxo Complexes Containing the Hydrotris(1-pyrazolyl)borate Ligand. *Organometallics* **2000**, *19*, 3957–3962. [CrossRef]
12. De Montigny, F.; Guy, L.; Pilet, G.; Vanthuyne, N.; Roussel, C.; Lombardi, R.; Freedman, T.B.; Nafie, L.A.; Crassous, J. Subtle chirality in oxo- and sulfidorhenium(v) complexes. *Chem. Commun.* **2009**, *32*, 4841–4843. [CrossRef] [PubMed]
13. Procopio, E.Q.; Dova, D.; Cauteruccio, S.; Forni, A.; Licandro, E.; Panigati, M. Dirhenium Coordination Complex Endowed with an Intrinsically Chiral Helical-Shaped Diphosphine Oxide. *ACS Omega* **2018**, *3*, 11649–11654. [CrossRef] [PubMed]
14. Slate, A.J.; Shalamanova, L.; Akhidime, I.D.; Whitehead, K.A. Rhenium and yttrium ions as antimicrobial agents against multidrug resistant Klebsiella pneumoniae and Acinetobacter baumannii biofilms. *Lett. Appl. Microbiol.* **2019**, *69*, 168–174. [CrossRef]
15. Kama, D.V.; Frei, A.; Brink, A.; Braband, H.; Alberto, R.; Roodt, A. New approach for the synthesis of water soluble *fac*-$[M^{I}(CO)_3]^+$ bis(diarylphosphino)alkylamine complexes (M = ^{99}Tc, Re). *Dalton Trans.* **2021**, *50*, 17506–17514. [CrossRef]
16. Frei, A.; Amado, M.; Cooper, M.A.; Blaskovich, M.A.T. Light-Activated Rhenium Complexes with Dual Mode of Action against Bacteria. *Chem. Eur. J.* **2020**, *26*, 2852–2858. [CrossRef] [PubMed]
17. Miller, R.G.; Vazquez-Hernandez, M.; Prochnow, P.; Bandow, J.E.; Metzler-Nolte, N. A CuAAC Click Approach for the Introduction of Bidentate Metal Complexes to a Sulfanilamide-Derived Antibiotic Fragment. *Inorg. Chem.* **2019**, *58*, 9404–9413. [CrossRef]
18. Pagoni, C.-C.; Xylouri, V.-S.; Kaiafas, G.C.; Lazou, M.; Bompola, G.; Tsoukas, E.; Papadopoulou, L.C.; Psomas, G.; Papagiannopoulou, D. Organometallic rhenium tricarbonyl–enrofloxacin and –levofloxacin complexes: Synthesis, albumin-binding, DNA-interaction and cell viability studies. *J. Biol. Inorg. Chem.* **2019**, *24*, 609–619. [CrossRef]
19. Wenzel, M.; Patra, M.; Senges, C.H.; Ott, I.; Stepanek, J.J.; Pinto, A.; Prochnow, P.; Vuong, C.; Langklotz, S.; Metzler-Nolte, N.; et al. Analysis of the mechanism of action of potent antibacterial hetero-tri-organometallic compounds: A structurally new class of antibiotics. *ACS Chem. Biol.* **2013**, *8*, 1442–1450. [CrossRef]
20. Siegmund, D.; Lorenz, N.; Gothe, Y.; Spies, C.; Geissler, B.; Prochnow, P.; Nuernberger, P.; Bandow, J.E.; Metzler-Nolte, N. Benzannulated Re(i)–NHC complexes: Synthesis, photophysical properties and antimicrobial activity. *Dalton Trans.* **2017**, *46*, 15269–15279. [CrossRef]
21. Cooper, S.M.; Siakalli, C.; White, A.J.P.; Frei, A.; Miller, P.W.; Long, N.J. Synthesis and anti-microbial activity of a new series of bis(diphosphine) rhenium(v) dioxo complexes. *Dalton Trans.* **2022**, *51*, 12791–12795. [CrossRef] [PubMed]
22. Mendes, S.S.; Marques, J.; Mesterházy, E.; Straetener, J.; Arts, M.; Pissarro, T.; Reginold, J.; Berscheid, A.; Bornikoel, J.; Kluj, R.M.; et al. Synergetic Antimicrobial Activity and Mechanism of Clotrimazole-Linked CO-Releasing Molecules. *ACS Bio Med Chem Au* **2022**, *2*, 419–436. [CrossRef] [PubMed]
23. Schindler, K.; Zobi, F. Anticancer and Antibiotic Rhenium Tri- and Dicarbonyl Complexes: Current Research and Future Perspectives. *Molecules* **2022**, *27*, 539. [CrossRef]

24. Huang, Z.; Wilson, J.J. Therapeutic and Diagnostic Applications of Multimetallic Rhenium(I) Tricarbonyl Complexes. *Eur. J. Inorg. Chem.* **2021**, *2021*, 1312–1324. [CrossRef]
25. Mkhatshwa, M.; Moremi, J.M.; Makgopa, K.; Manicum, A.-L.E. Nanoparticles Functionalised with Re(I) Tricarbonyl Complexes for Cancer Theranostics. *Int. J. Mol. Sci.* **2021**, *22*, 6546. [CrossRef] [PubMed]
26. Liew, H.S.; Mai, C.-W.; Zulkefeli, M.; Madheswaran, T.; Kiew, L.V.; Delsuc, N.; Low, M.L. Recent Emergence of Rhenium(I) Tricarbonyl Complexes as Photosensitisers for Cancer Therapy. *Molecules* **2020**, *25*, 4176. [CrossRef]
27. Collery, P.; Desmaele, D.; Vijaykumar, V. Design of Rhenium Compounds in Targeted Anticancer Therapeutics. *Curr. Pharm. Des.* **2019**, *25*, 3306–3322. [CrossRef]
28. Bauer, E.B.; Haase, A.A.; Reich, R.M.; Crans, D.C.; Kühn, F.E. Organometallic and coordination rhenium compounds and their potential in cancer therapy. *Coord. Chem. Rev.* **2019**, *393*, 79–117. [CrossRef]
29. Konkankit, C.C.; Marker, S.C.; Knopf, K.M.; Wilson, J.J. Anticancer activity of complexes of the third row transition metals, rhenium, osmium, and iridium. *Dalton Trans.* **2018**, *47*, 9934–9974. [CrossRef]
30. Lee, L.C.; Leung, K.K.; Lo, K.K. Recent development of luminescent rhenium(I) tricarbonyl polypyridine complexes as cellular imaging reagents, anticancer drugs, and antibacterial agents. *Dalton Trans.* **2017**, *46*, 16357–16380. [CrossRef]
31. Leonidova, A.; Gasser, G. Underestimated Potential of Organometallic Rhenium Complexes as Anticancer Agents. *ACS Chem. Biol.* **2014**, *9*, 2180–2193. [CrossRef] [PubMed]
32. Sharma, A.; Vaibhavi, N.; Kar, B.; Das, U.; Paira, P. Target-specific mononuclear and binuclear rhenium(i) tricarbonyl complexes as upcoming anticancer drugs. *RSC Adv.* **2022**, *12*, 20264–20295. [CrossRef] [PubMed]
33. Karges, J.; Kalaj, M.; Gembicky, M.; Cohen, S.M. ReI Tricarbonyl Complexes as Coordinate Covalent Inhibitors for the SARS-CoV-2 Main Cysteine Protease. *Angew. Chem. Int. Ed.* **2021**, *60*, 10716–10723. [CrossRef] [PubMed]
34. Valentová, J.; Lintnerová, L. Chirality in Anticancer Agents. In *Current Topics in Chirality*; Takashiro, A., Ed.; IntechOpen: Rijeka, Croatia, 2021; Volume Chapter 8. [CrossRef]
35. Atilla-Gokcumen, G.E.; Williams, D.S.; Bregman, H.; Pagano, N.; Meggers, E. Organometallic Compounds with Biological Activity: A Very Selective and Highly Potent Cellular Inhibitor for Glycogen Synthase Kinase 3. *Chembiochem* **2006**, *7*, 1443–1450. [CrossRef] [PubMed]
36. Silvestri, I.P.; Colbon, P.J.J. The Growing Importance of Chirality in 3D Chemical Space Exploration and Modern Drug Discovery Approaches for Hit-ID. *ACS Med. Chem. Lett.* **2021**, *12*, 1220–1229. [CrossRef] [PubMed]
37. Suárez-Ortiz, G.A.; Hernández-Correa, R.; Morales-Moreno, M.D.; Toscano, R.A.; Ramirez-Apan, M.T.; Hernandez-Garcia, A.; Amézquita-Valencia, M.; Araiza-Olivera, D. Diastereomeric Separation of Chiral *fac*-Tricarbonyl(iminopyridine) Rhenium(I) Complexes and Their Cytotoxicity Studies: Approach toward an Action Mechanism against Glioblastoma. *J. Med. Chem.* **2022**, *65*, 9281–9294. [CrossRef]
38. Rossier, J.; Hauser, D.; Kottelat, E.; Rothen-Rutishauser, B.; Zobi, F. Organometallic cobalamin anticancer derivatives for targeted prodrug delivery via transcobalamin-mediated uptake. *Dalton Trans.* **2017**, *46*, 2159–2164. [CrossRef]
39. Marker, S.C.; MacMillan, S.N.; Zipfel, W.R.; Li, Z.; Ford, P.C.; Wilson, J.J. Photoactivated in Vitro Anticancer Activity of Rhenium(I) Tricarbonyl Complexes Bearing Water-Soluble Phosphines. *Inorg. Chem.* **2018**, *57*, 1311–1331. [CrossRef]
40. Muñoz-Osses, M.; Siegmund, D.; Gómez, A.; Godoy, F.; Fierro, A.; Llanos, L.; Aravena, D.; Metzler-Nolte, N. Influence of the substituent on the phosphine ligand in novel rhenium(i) aldehydes. Synthesis, computational studies and first insights into the antiproliferative activity. *Dalton Trans.* **2018**, *47*, 13861–13869. [CrossRef]
41. Schutte-Smith, M.; Marker, S.C.; Wilson, J.J.; Visser, H.G. Aquation and Anation Kinetics of Rhenium(I) Dicarbonyl Complexes: Relation to Cell Toxicity and Bioavailability. *Inorg. Chem.* **2020**, *59*, 15888–15897. [CrossRef]
42. Delasoie, J.; Schiel, P.; Vojnovic, S.; Nikodinovic-Runic, J.; Zobi, F. Photoactivatable Surface-Functionalized Diatom Microalgae for Colorectal Cancer Targeted Delivery and Enhanced Cytotoxicity of Anticancer Complexes. *Pharmaceutics* **2020**, *12*, 480. [CrossRef] [PubMed]
43. Sovari, S.N.; Radakovic, N.; Roch, P.; Crochet, A.; Pavic, A.; Zobi, F. Combatting AMR: A molecular approach to the discovery of potent and non-toxic rhenium complexes active against C. albicans-MRSA co-infection. *Eur. J. Med. Chem.* **2021**, *226*, 113858. [CrossRef] [PubMed]
44. Sovari, S.N.; Vojnovic, S.; Bogojevic, S.S.; Crochet, A.; Pavic, A.; Nikodinovic-Runic, J.; Zobi, F. Design, synthesis and in vivo evaluation of 3-arylcoumarin derivatives of rhenium(I) tricarbonyl complexes as potent antibacterial agents against methicillin-resistant Staphylococcus aureus (MRSA). *Eur. J. Med. Chem.* **2020**, *205*, 112533. [CrossRef] [PubMed]
45. Prieto, L.; Rossier, J.; Derszniak, K.; Dybas, J.; Oetterli, R.M.; Kottelat, E.; Chlopicki, S.; Zelder, F.; Zobi, F. Modified biovectors for the tuneable activation of anti-platelet carbon monoxide release. *Chem. Commun.* **2017**, *53*, 6840–6843. [CrossRef] [PubMed]
46. Santoro, G.; Beltrami, R.; Kottelat, E.; Blacque, O.; Bogdanova, A.Y.; Zobi, F. N-Nitrosamine-{cis-Re$[CO]_2\}^{2+}$ cobalamin conjugates as mixed CO/NO-releasing molecules. *Dalton Trans.* **2016**, *45*, 1504–1513. [CrossRef] [PubMed]
47. Suliman, H.B.; Zobi, F.; Piantadosi, C.A. Heme Oxygenase-1/Carbon Monoxide System and Embryonic Stem Cell Differentiation and Maturation into Cardiomyocytes. *Antioxid. Redox Signal.* **2016**, *24*, 345–360. [CrossRef]
48. Schindler, K.; Crochet, A.; Zobi, F. Aerobically stable and substitutionally labile α-diimine rhenium dicarbonyl complexes. *RSC Adv.* **2021**, *11*, 7511–7520. [CrossRef]

49. Romashev, N.F.; Abramov, P.A.; Bakaev, I.V.; Fomenko, I.S.; Samsonenko, D.G.; Novikov, A.S.; Tong, K.K.H.; Ahn, D.; Dorovatovskii, P.V.; Zubavichus, Y.V.; et al. Heteroleptic Pd(II) and Pt(II) Complexes with Redox-Active Ligands: Synthesis, Structure, and Multimodal Anticancer Mechanism. *Inorg. Chem.* **2022**, *61*, 2105–2118. [CrossRef]
50. Biancalana, L.; Batchelor, L.K.; Dyson, P.J.; Zacchini, S.; Schoch, S.; Pampaloni, G.; Marchetti, F. α-Diimine homologues of cisplatin: Synthesis, speciation in DMSO/water and cytotoxicity. *New J. Chem.* **2018**, *42*, 17453–17463. [CrossRef]
51. Yambulatov, D.S.; Lutsenko, I.A.; Nikolaevskii, S.A.; Petrov, P.A.; Smolyaninov, I.V.; Malyants, I.K.; Shender, V.O.; Kiskin, M.A.; Sidorov, A.A.; Berberova, N.T.; et al. α-Diimine Cisplatin Derivatives: Synthesis, Structure, Cyclic Voltammetry and Cytotoxicity. *Molecules* **2022**, *27*, 8565.
52. Amoroso, A.J.; Coogan, M.P.; Dunne, J.E.; Fernández-Moreira, V.; Hess, J.B.; Hayes, A.J.; Lloyd, D.; Millet, C.; Pope, S.J.A.; Williams, C. Rhenium fac tricarbonyl bisimine complexes: Biologically useful fluorochromes for cell imaging applications. *Chem. Commun.* **2007**, *29*, 3066–3068. [CrossRef] [PubMed]
53. Louie, M.-W.; Ho-Chuen Lam, M.; Kam-Wing Lo, K. Luminescent Polypyridinerhenium(I) Bis-Biotin Complexes as Crosslinkers for Avidin. *Eur. J. Inorg. Chem.* **2009**, *2009*, 4265–4273. [CrossRef]
54. Leonidova, A.; Pierroz, V.; Adams, L.A.; Barlow, N.; Ferrari, S.; Graham, B.; Gasser, G. Enhanced Cytotoxicity through Conjugation of a "Clickable" Luminescent Re(I) Complex to a Cell-Penetrating Lipopeptide. *ACS Med. Chem. Lett.* **2014**, *5*, 809–814. [CrossRef] [PubMed]
55. Ye, R.R.; Tan, C.P.; Chen, M.H.; Hao, L.; Ji, L.N.; Mao, Z.W. Mono- and Dinuclear Phosphorescent Rhenium(I) Complexes: Impact of Subcellular Localization on Anticancer Mechanisms. *Chem. Eur. J.* **2016**, *22*, 7800–7809. [CrossRef] [PubMed]
56. Clede, S.; Lambert, F.; Saint-Fort, R.; Plamont, M.A.; Bertrand, H.; Vessieres, A.; Policar, C. Influence of the Side-Chain Length on the Cellular Uptake and the Cytotoxicity of Rhenium Triscarbonyl Derivatives: A Bimodal Infrared and Luminescence Quantitative Study. *Chem. Eur. J.* **2014**, *20*, 8714–8722. [CrossRef] [PubMed]
57. Quan, L.; Sun, T.; Lin, W.; Guan, X.; Zheng, M.; Xie, Z.; Jing, X. BODIPY Fluorescent Chemosensor for Cu2+ Detection and Its Applications in Living Cells: Fast Response and High Sensitivity. *J. Fluoresc.* **2014**, *24*, 841–846. [CrossRef] [PubMed]
58. Potocny, A.M.; Teesdale, J.J.; Marangoz, A.; Yap, G.P.A.; Rosenthal, J. Spectroscopic and $^1O_2$ Sensitization Characteristics of a Series of Isomeric Re(bpy)$(CO)_3$Cl Complexes Bearing Pendant BODIPY Chromophores. *Inorg. Chem.* **2019**, *58*, 5042–5050. [CrossRef]
59. Teesdale, J.J.; Pistner, A.J.; Yap, G.P.A.; Ma, Y.-Z.; Lutterman, D.A.; Rosenthal, J. Reduction of CO_2 using a rhenium bipyridine complex containing ancillary BODIPY moieties. *Catal. Today* **2014**, *225*, 149–157. [CrossRef]
60. Andrade, G.A.; Pistner, A.J.; Yap, G.P.A.; Lutterman, D.A.; Rosenthal, J. Photocatalytic Conversion of CO_2 to CO Using Rhenium Bipyridine Platforms Containing Ancillary Phenyl or BODIPY Moieties. *ACS Catal.* **2013**, *3*, 1685–1692. [CrossRef]
61. Schindler, K.; Cortat, Y.; Nedyalkova, M.; Crochet, A.; Lattuada, M.; Pavic, A.; Zobi, F. Antimicrobial Activity of Rhenium Di- and Tricarbonyl Diimine Complexes: Insights on Membrane-Bound S. aureus Protein Binding. *Pharmaceuticals* **2022**, *15*, 1107. [CrossRef]
62. Kitanovic, I.; Can, S.Z.; Alborzinia, H.; Kitanovic, A.; Pierroz, V.; Leonidova, A.; Pinto, A.; Spingler, B.; Ferrari, S.; Molteni, R.; et al. A Deadly Organometallic Luminescent Probe: Anticancer Activity of a ReI Bisquinoline Complex. *Chem. Eur. J.* **2014**, *20*, 2496–2507. [CrossRef] [PubMed]
63. Knopf, K.M.; Murphy, B.L.; MacMillan, S.N.; Baskin, J.M.; Barr, M.P.; Boros, E.; Wilson, J.J. In Vitro Anticancer Activity and in Vivo Biodistribution of Rhenium(I) Tricarbonyl Aqua Complexes. *J. Am. Chem. Soc.* **2017**, *139*, 14302–14314. [CrossRef] [PubMed]
64. König, M.; Siegmund, D.; Raszeja, L.J.; Prokop, A.; Metzler-Nolte, N. Resistance-breaking profiling and gene expression analysis on an organometallic ReI–phenanthridine complex reveal parallel activation of two apoptotic pathways. *Med. Chem. Commun.* **2018**, *9*, 173–180. [CrossRef] [PubMed]
65. Konkankit, C.C.; King, A.P.; Knopf, K.M.; Southard, T.L.; Wilson, J.J. In Vivo Anticancer Activity of a Rhenium(I) Tricarbonyl Complex. *ACS Med. Chem. Lett.* **2019**, *10*, 822–827. [CrossRef] [PubMed]
66. Wang, F.X.; Liang, J.H.; Zhang, H.; Wang, Z.H.; Wan, Q.; Tan, C.P.; Ji, L.N.; Mao, Z.W. Mitochondria-Accumulating Rhenium(I) Tricarbonyl Complexes Induce Cell Death via Irreversible Oxidative Stress and Glutathione Metabolism Disturbance. *ACS Appl. Mater. Interfaces* **2019**, *11*, 13123–13133. [CrossRef]
67. Munoz-Osses, M.; Godoy, F.; Fierro, A.; Gomez, A.; Metzler-Nolte, N. New organometallic imines of rhenium(I) as potential ligands of GSK-3 beta: Synthesis, characterization and biological studies. *Dalton Trans.* **2018**, *47*, 1233–1242. [CrossRef]
68. Kaplanis, M.; Stamatakis, G.; Papakonstantinou, V.D.; Paravatou-Petsotas, M.; Demopoulos, C.A.; Mitsopoulou, C.A. Re(I) tricarbonyl complex of 1,10-phenanthroline-5,6-dione: DNA binding, cytotoxicity, anti-inflammatory, and anti-coagulant effects towards platelet activating factor. *J. Inorg. Biochem.* **2014**, *135*, 1–9. [CrossRef]
69. Balakrishnan, G.; Rajendran, T.; Senthil Murugan, K.; Sathish Kumar, M.; Sivasubramanian, V.K.; Ganesan, M.; Mahesh, A.; Thirunalasundari, T.; Rajagopal, S. Interaction of rhenium(I) complex carrying long alkyl chain with Calf Thymus DNA: Cytotoxic and cell imaging studies. *Inorg. Chim. Acta* **2015**, *434*, 51–59. [CrossRef]
70. Zobi, F.; Spingler, B.; Alberto, R. Guanine and plasmid DNA binding of mono- and trinuclear *fac*-$[Re(CO)_3]^+$ complexes with amino acid Ligands. *Chembiochem* **2005**, *6*, 1397–1405. [CrossRef]
71. Caspar, J.V.; Sullivan, B.P.; Meyer, T.J. Synthetic Routes to Luminescent 2,2′-Bipyridyl Complexes of Rhenium—Preparation and Spectral and Redox Properties of Mono(Bipyridyl) Complexes of Rhenium(Iii) and Rhenium(I). *Inorg. Chem.* **1984**, *23*, 2104–2109. [CrossRef]

72. Smithback, J.L.; Helms, J.B.; Schutte, E.; Woessner, S.M.; Sullivan, B.P. Preparative Routes to Luminescent Mixed-Ligand Rhenium(I) Dicarbonyl Complexes. *Inorg. Chem.* **2006**, *45*, 2163–2174. [CrossRef] [PubMed]
73. Skiba, J.; Kowalczyk, A.; Stączek, P.; Bernaś, T.; Trzybiński, D.; Woźniak, K.; Schatzschneider, U.; Czerwieniec, R.; Kowalski, K. Luminescent *fac*-[Re(CO)$_3$(phen)] carboxylato complexes with non-steroidal anti-inflammatory drugs: Synthesis and mechanistic insights into the in vitro anticancer activity of *fac*-[Re(CO)$_3$(phen)(aspirin)]. *New J. Chem.* **2019**, *43*, 573–583. [CrossRef]
74. Ragone, F.; Saavedra, H.H.M.; Gara, P.M.D.; Ruiz, G.T.; Wolcan, E. Photosensitized Generation of Singlet Oxygen from Re(I) Complexes: A Photophysical Study Using LIOAS and Luminescence Techniques. *J. Phys. Chem. A* **2013**, *117*, 4428–4435. [CrossRef] [PubMed]
75. Cuesta, L.; Hevia, E.; Morales, D.; Pérez, J.; Riera, L.; Miguel, D. Reactivity of Molybdenum and Rhenium Hydroxo Complexes toward Organic Electrophiles: Reactions that Afford Carboxylato Products. *Organometallics* **2006**, *25*, 1717–1722. [CrossRef]
76. Kisel, K.S.; Melnikov, A.S.; Grachova, E.V.; Hirva, P.; Tunik, S.P.; Koshevoy, I.O. Linking ReI and PtII Chromophores with Aminopyridines: A Simple Route to Achieve a Complicated Photophysical Behavior. *Chem. Eur. J.* **2017**, *23*, 11301–11311. [CrossRef] [PubMed]
77. Hevia, E.; Pérez, J.; Riera, V.; Miguel, D. New Octahedral Rhenium(I) Tricarbonyl Amido Complexes. *Organometallics* **2002**, *21*, 1966–1974. [CrossRef]
78. Cuesta, L.; Huertos, M.A.; Morales, D.; Pérez, J.; Riera, L.; Riera, V.; Miguel, D.; Menéndez-Velázquez, A.; García-Granda, S. Synthesis, Structure, and Reactivity of Mononuclear Re(I) Oximato Complexes. *Inorg. Chem.* **2007**, *46*, 2836–2845. [CrossRef]
79. Coogan, M.P.; Platts, J.A. Blue rhenium tricarbonyl DPPZ complexes—Low energy charge-transfer absorption at tissue-penetrating wavelengths. *Chem. Commun.* **2016**, *52*, 12498–12501. [CrossRef]
80. Capper, M.S.; Enriquez Garcia, A.; Macia, N.; Lai, B.; Lin, J.-B.; Nomura, M.; Alihosseinzadeh, A.; Ponnurangam, S.; Heyne, B.; Shemanko, C.S.; et al. Cytotoxicity, cellular localization and photophysical properties of Re(I) tricarbonyl complexes bound to cysteine and its derivatives. *J. Biol. Inorg. Chem.* **2020**, *25*, 759–776. [CrossRef]
81. Cañadas, P.; Ziegler, S.; Fombona, S.; Hevia, E.; Miguel, D.; Pérez, J.; Riera, L. Molybdenum and rhenium carbonyl complexes containing thiolato ligands. *J. Organomet. Chem.* **2019**, *896*, 113–119. [CrossRef]
82. Hayoz, P.; von Zelewsky, A. New versatile optically active bipyridines as building blocks for helicating and caging ligands. *Tetrahedron Lett.* **1992**, *33*, 5165–5168. [CrossRef]
83. Abram, U.; Hübener, R.; Alberto, R.; Schibli, R. Darstellung und Strukturen von (Et$_4$N)$_2$[Re(CO)$_3$(NCS)$_3$] und (Et$_4$N)[Re(CO)$_2$Br$_4$]. *Z. Anorg. Allg. Chem.* **1996**, *622*, 813–818. [CrossRef]
84. De Clercq, E.; Field, H.J. Antiviral prodrugs—The development of successful prodrug strategies for antiviral chemotherapy. *Br. J. Pharmacol.* **2006**, *147*, 1–11. [CrossRef]
85. Collery, P.; Mohsen, A.; Kermagoret, A.; Corre, S.; Bastian, G.; Tomas, A.; Wei, M.; Santoni, F.; Guerra, N.; Desmaele, D.; et al. Antitumor activity of a rhenium (I)-diselenoether complex in experimental models of human breast cancer. *Investig. New Drugs* **2015**, *33*, 848–860. [CrossRef] [PubMed]
86. Zobi, F.; Alberto, R. Redox-Induced Binding of [(tacn)ReBr^{II}(CO)$_2$]$^+$ to Guanine, Oligonucleotides, and Peptides. *Chem. Eur. J.* **2010**, *16*, 2710–2713. [CrossRef] [PubMed]
87. Zobi, F.; Blacque, O.; Sigel, R.K.O.; Alberto, R. Binding interaction of [Re(H$_2$O)$_3$(CO)$_3$]$^+$ with the DNA fragment d(CpGpG). *Inorg. Chem.* **2007**, *46*, 10458–10460. [CrossRef] [PubMed]
88. Adams, K.M.; Marzilli, L.G. *fac*-[Re(CO)$_3$(H$_2$O)$_3$]$^+$ Nucleoside Monophosphate Adducts Investigated in Aqueous Solution by Multinuclear NMR Spectroscopy. *Inorg. Chem.* **2007**, *46*, 4926–4936. [CrossRef]
89. Oriskovich, T.A.; White, P.S.; Thorp, H.H. Luminescent Labels for Purine Nucleobases: Electronic Properties of Guanine Bound to Rhenium(I). *Inorg. Chem.* **1995**, *34*, 1629–1631. [CrossRef]
90. Williams, J.D.; Kampmeier, F.; Badar, A.; Howland, K.; Cooper, M.S.; Mullen, G.E.D.; Blower, P.J. Optimal His-Tag Design for Efficient [^{99m}Tc(CO)$_3$]$^+$ and [^{188}Re(CO)$_3$]$^+$ Labeling of Proteins for Molecular Imaging and Radionuclide Therapy by Analysis of Peptide Arrays. *Bioconjugate Chem.* **2021**, *32*, 1242–1254. [CrossRef]
91. Pospíšil, P.; Sýkora, J.; Takematsu, K.; Hof, M.; Gray, H.B.; Vlček, A. Light-Induced Nanosecond Relaxation Dynamics of Rhenium-Labeled Pseudomonas aeruginosa Azurins. *J. Phys. Chem. B* **2020**, *124*, 788–797. [CrossRef]
92. De Tommaso, G.; Celentano, V.; Malgieri, G.; Fattorusso, R.; Romanelli, A.; D'Andrea, L.D.; Iuliano, M.; Isernia, C. *fac*-[Re(H$_2$O)$_3$(CO)$_3$]$^+$ Complexed with Histidine and Imidazole in Aqueous Solution: Speciation, Affinity and Binding Features. *ChemistrySelect* **2016**, *1*, 3739–3744. [CrossRef]
93. Simpson, E.J.; Hickey, J.L.; Breadner, D.; Luyt, L.G. Investigation of isomer formation upon coordination of bifunctional histidine analogues with 99mTc/Re(CO)3. *Dalton Trans.* **2012**, *41*, 2950–2958. [CrossRef] [PubMed]
94. Binkley, S.L.; Leeper, T.C.; Rowlett, R.S.; Herrick, R.S.; Ziegler, C.J. Re(CO)$_3$(H$_2$O)$_3$$^+$ binding to lysozyme: Structure and reactivity. *Metallomics* **2011**, *3*, 909–916. [CrossRef] [PubMed]
95. Papagiannopoulou, D.; Tsoukalas, C.; Makris, G.; Raptopoulou, C.P.; Psycharis, V.; Leondiadis, L.; Gniazdowska, E.; Koźmiński, P.; Fuks, L.; Pelecanou, M.; et al. Histidine derivatives as tridentate chelators for the *fac*-[M^I(CO)$_3$] (Re, ^{99}mTc, ^{188}Re) core: Synthesis, structural characterization, radiochemistry and stability. *Inorg. Chim. Acta* **2011**, *378*, 333–337. [CrossRef]
96. Herrick, R.S.; Ziegler, C.J.; Gambella, A. Reactions of [Re(CO)$_3$]$^+$ with Histidylhistidine and Modified Histidines. *Eur. J. Inorg. Chem.* **2010**, *2010*, 3905–3908. [CrossRef]

97. Zobi, F.; Kromer, L.; Spingler, B.; Alberto, R. Synthesis and Reactivity of the 17 e^- Complex $[Re^{II}Br_4(CO)_2]^{2-}$: A Convenient Entry into Rhenium(II) Chemistry. *Inorg. Chem.* **2009**, *48*, 8965–8970. [CrossRef]
98. Kolp, B.; Abeln, D.; Stoeckli-Evans, H.; von Zelewsky, A. Platinum(II) Compounds with Enantiomerically Pure Bis(pinene)-Fused Bipyridine Ligands − Diimine-Dichloro Complexes and Their Substitution Reactions. *Eur. J. Inorg. Chem.* **2001**, *2001*, 1207–1220. [CrossRef]
99. Sheldrick, G.M. Crystal structure refinement with SHELXL. *Acta Cryst. C* **2015**, *71*, 3–8. [CrossRef]
100. Sheldrick, G.M. SHELXT—Integrated space-group and crystal-structure determination. *Acta Cryst. A* **2015**, *71*, 3–8. [CrossRef]